

Multiple quantum phases in artificial double-dot molecules

Massimo Rontani^{1,2}, F. Rossi^{1,2,3}, F. Manghi^{1,2}, and E. Molinari^{1,2}

¹ *Istituto Nazionale per la Fisica della Materia (INFM)*

² *Dipartimento di Fisica, Università di Modena e Reggio Emilia, Via Campi 213/A, I-41100 Modena, Italy*

³ *Dipartimento di Fisica, Politecnico di Torino, Corso Duca degli Abruzzi 24, I-10129 Torino, Italy*

(17 June 1999)

We study coupled semiconductor quantum dots theoretically through a generalized Hubbard approach, where intra- and inter-dot Coulomb correlation, as well as tunneling effects are described on the basis of realistic electron wavefunctions. We find that the ground-state configuration of vertically-coupled double dots undergoes non-trivial quantum transitions as a function of the inter-dot distance d ; at intermediate values of d we predict a new phase that should be observable in the addition spectra and in the magnetization changes.

Semiconductor quantum dots (QDs) are nano- or mesoscopic structures that can be regarded as ‘artificial atoms’ because of the three-dimensional carrier confinement and the resulting discrete energy spectrum. They are currently receiving great attention because they can be designed to study and exploit new physical phenomena: On the one hand, the nature and scale of electronic confinement allows the exploration of regimes that are not accessible in conventional atomic physics; on the other hand, they lead to novel devices dominated by single- or few-electron effects [1,2].

One of the important challenges at this point is to understand the fundamental properties of coupled quantum dots, the simplest structures that display the interactions controlling potential quantum-computing devices. Here also the interdot coupling can be tuned through external parameters, far out of the regimes known in ‘natural molecules’ where the ground-state interatomic distance is dictated by the nature of bonding. We expect that new phenomena will occur in these ‘artificial molecules’ (AMs) when the relative importance of Coulomb interaction and single-particle tunneling is varied. Through the study of such phenomena, coupled dots may become a unique laboratory to explore electronic correlations.

In this paper we analyze ground and excited few-particle states of realistic double quantum dots (DQDs) using a theoretical scheme that fully takes into account intra- and inter-dot many-body interactions. We focus on strongly confined vertically-coupled DQDs, and show that, for a given number of electrons, N , the ground state configuration undergoes non-trivial quantum transitions as a function of the inter-dot distance d ; we identify specific ranges of the DQD parameters characterizing a ‘coherent’ molecular phase, where tunneling effects

dominate, and a phase where the inter-dot interaction is purely electrostatic. At intermediate values of d we predict a new phase that should be observable by means of transport experiments in the addition spectra and in the magnetization changes.

From the theoretical point of view, a major difficulty is that we cannot make use of perturbative schemes [3] in the calculation of the DQD many-body ground state, since we want to investigate all inter-dot coupling regimes. We thus write the many-body hamiltonian H within a generalized Hubbard (GHH) approach [4], and chose a basis set formed by suitable single-particle wavefunctions localized on either dot ($i = 1, 2$), and characterized by orbital quantum numbers, α (to be specified below), and by the spin quantum number, σ . On this basis the many-body hamiltonian is

$$\hat{H} = \sum_{i\alpha\sigma} \tilde{\epsilon}_\alpha \hat{n}_{i\alpha\sigma} - t \sum_{\alpha\sigma\langle ij \rangle} \hat{c}_{i\alpha\sigma}^\dagger \hat{c}_{j\alpha\sigma} + \frac{1}{2} \sum_{i\alpha\beta\sigma} U_{\alpha\beta} \hat{n}_{i\alpha\sigma} \hat{n}_{i\beta-\sigma} + \frac{1}{2} \sum_{i\alpha\beta\sigma} (U_{\alpha\beta} - J_{\alpha\beta}) \hat{n}_{i\alpha\sigma} \hat{n}_{i\beta\sigma} + \sum_{\alpha\beta\sigma\sigma'} \tilde{U}_{\alpha\beta} \hat{n}_{1\alpha\sigma} \hat{n}_{2\beta\sigma'}.$$

The first two addenda are the single-particle on-site and hopping term respectively: $\tilde{\epsilon}_\alpha$ are the single-particle energies, t the tunneling parameter; \hat{n} are the occupation numbers and \hat{c} (\hat{c}^\dagger) the creation (destruction) operators. The third and fourth terms account for intra-dot Coulomb interaction between electrons with antiparallel and parallel spins, respectively: U and J are the intra-dot Coulomb and exchange integrals. Finally, the last term represents the inter-dot Coulomb coupling, \tilde{U} being the inter-dot Coulomb integrals. These integrals are in turn expressed in terms of single-particle states:

$$U_{\alpha\beta} = \int \frac{e^2 |\phi_{i\alpha}(\mathbf{r})|^2 |\phi_{i\beta}(\mathbf{r}')|^2}{\kappa_r |\mathbf{r} - \mathbf{r}'|} d\mathbf{r} d\mathbf{r}';$$

$$\tilde{U}_{\alpha\beta} = \int \frac{e^2 |\phi_{1\alpha}(\mathbf{r})|^2 |\phi_{2\beta}(\mathbf{r}')|^2}{\kappa_r |\mathbf{r} - \mathbf{r}'|} d\mathbf{r} d\mathbf{r}';$$

$$J_{\alpha\beta} = \int \frac{e^2 \phi_{i\alpha}^*(\mathbf{r}) \phi_{i\beta}^*(\mathbf{r}') \phi_{i\alpha}(\mathbf{r}') \phi_{i\beta}(\mathbf{r})}{\kappa_r |\mathbf{r} - \mathbf{r}'|} d\mathbf{r} d\mathbf{r}';$$

with $\phi_{i\alpha}(\mathbf{r})$ full three-dimensional single-particle wavefunctions (obtained within the usual envelope-function approximation), e electronic charge and κ_r relative dielectric constant.

Here we shall consider a specific type of nanostructures, namely vertically coupled cylindrical DQDs [5]; the ingredients entering the Hamiltonian can therefore be defined explicitly. For simplicity, $V(r)$ can be assumed to be separable in the xy and z components; the profile is taken to be parabolic in the xy plane, with confinement energy $\hbar\omega$, and a symmetric double quantum well (QW) along z [5,6]. The eigenstates of the xy harmonic potential are the usual Fock-Darwin states $|\alpha\rangle = |(n, m)\rangle$ (n, m radial and angular quantum numbers) [2]. Along z , the QW thickness is such that only the lowest eigenstates (symmetric, $|s\rangle$, and antisymmetric $|a\rangle$) are relevant for the low-energy spectrum. From these, we construct a complete set of states that are localized on either dot (see inset of Fig. 1): $|1\rangle = (|s\rangle + |a\rangle)/\sqrt{2}$ and $|2\rangle = (|s\rangle - |a\rangle)/\sqrt{2}$. The basis we use is therefore the direct product $|\alpha\sigma\rangle = |i\rangle \otimes |\alpha\rangle \otimes |\sigma\rangle$. The single-particle energies are $\tilde{\epsilon}_\alpha = \epsilon_\alpha + (\epsilon_s + \epsilon_a)/2$, and the tunneling parameter is $t = (\epsilon_a - \epsilon_s)/2$, with ϵ_s, ϵ_a double-well eigenenergies, and ϵ_α oscillator energies.

Using the above expressions, the three-dimensional Coulomb integrals and the tunneling parameter are computed directly from the single-particle states for each sample. Fig. 1 shows the result for t , $U_{\alpha\beta}$ and $\tilde{U}_{\alpha\beta}$ [$\alpha = \beta = (0, 0)$] calculated for a GaAs/AlAs DQD ($\kappa_r = 12.98$, effective mass $0.065 m_e$) with $\hbar\omega = 10$ meV, as a function of the interdot distance (barrier width) d . Note that already around $d = 5$ nm the inter-dot Coulomb integral exceeds the single-particle hopping parameter.

To obtain the many-body energies and eigenstates, the Hamiltonian \hat{H} is then diagonalized exactly for each value of N (total number of electrons) on each configuration subspace labeled by the quantum numbers S (z -component of the total spin) and M (z -component of the total angular momentum).

This approach has two main advantages: First, it allows us to solve the many-body problem consistently in the different coupling regimes, from the limit where t dominates over the Coulomb integrals to the opposite limit where t is negligible. Second, it can provide quantitative predictions for given DQD structures, since it contains no free parameters and uses realistic ingredients (t , $U_{\alpha\beta}$, $\tilde{U}_{\alpha\beta}$, $J_{\alpha\beta}$) calculated for each nanostructure [7].

Fig. 2 shows the calculated ground-state energies E_N of correlated N -particle states as a function of the interdot distance d [8]. The three lowest excited states are also shown for comparison. As expected, when d is large, the system behaves as two isolated QDs. With decreasing d , some of the many-body excited states, favoured by Coulomb interactions, become lower in energy. For $N \leq 3$ a single quantum phase transition occurs, below which the new ground state is a molecular-like state. For $N > 3$, two successive transitions take place, at $d = d_b$ and $d = d_a$, and an intermediate non-trivial phase is predicted to occur in the range $d_a < d < d_b$. Note that this phase is stable in a relatively large range of d values, which depends on the number of electrons. An accurate

determination of d_a and d_b requires the correct inclusion of all inter-dot coupling terms, including the inter-dot Coulomb integrals. If the latter are neglected, all quantum transitions occur for smaller values of the inter-dot distance, and the d -range of the intermediate phase is underestimated significantly; had also the other many body terms been neglected, the intermediate phase would disappear leaving a simple crossover from a molecular to an atomic like regime at $d = d_a = d_b$.

To understand the nature of the different phases it is useful to examine the many-body states in terms of the single Slater determinants that contribute to each of them. Here we discuss explicitly the 4-electron case with the help of the insets in Fig. 2, but the same reasoning can be followed for the other cases. Both in the case of very small and very large interdot distances the ground state can be essentially described in terms of a single Slater determinant: for large values of d ($d > d_b$), the relevant configurations for the ground state have two electrons in the lowest level of each isolated dot; the $|s\rangle$ and $|a\rangle$ extended ‘molecular’ orbitals derived from the lowest ‘atomic’ states are of course almost degenerate and both filled with two electrons. In the opposite limit ($d < d_a$), by expanding the localized atomic orbitals in terms of molecular orbitals we recognize that the $|s\rangle$ state derived from the lowest atomic state is filled with two electrons, while the corresponding $|a\rangle$ molecular state is empty. The two remaining electrons occupy the next bonding molecular orbitals—derived from the higher p_x and p_y levels—with parallel spin, in such a way that S is maximized. This is the manifestation of Coulomb interaction which leads to Hund’s rule for molecules.

In these two extreme phases the single particle picture is essentially correct, provided that the appropriate basis set (either localized or extended orbitals) is used. In the intermediate phase, $d_a < d < d_b$, this is no longer true and the ground state is a mixture of different Slater determinants in any basis set [9]. In this sense again the intermediate phase exhibits an intrinsic many-body character. Coulomb direct and exchange terms, responsible for the selection of the global quantum numbers, determine a new ground state configuration, where both S and M are maximized.

We obtain a clear evidence of the different electronic distribution in the three quantum phases by calculating the spin-dependent electronic pair correlation function, defined as

$$g_{\sigma', \sigma''}(\rho, z', z'') = \int d\mathbf{R} \langle \hat{\Psi}_{\sigma'}^\dagger(\mathbf{r}') \hat{\Psi}_{\sigma''}^\dagger(\mathbf{r}'') \hat{\Psi}_{\sigma''}(\mathbf{r}'') \hat{\Psi}_{\sigma'}(\mathbf{r}') \rangle,$$

where $\mathbf{R} = (\rho' + \rho'')/2$ and $\rho = (\rho' - \rho'')$. Here $\rho' = (x', y')$, $\rho'' = (x'', y'')$ are the in-plane spatial coordinates of the electrons in the pair, and z' and z'' are their coordinates along z , that will be kept fixed at the center of either QD, i.e. in z_1 or z_2 . $\mathbf{r}' = (\rho', z')$, $\mathbf{r}'' = (\rho'', z'')$. σ', σ'' are the spin variables and can assume the values \uparrow or \downarrow . In Fig. 3 we plot for example $g_{\downarrow, \downarrow}(x, y, z', z'')$ for a double QD with $N = 6$ electrons, at three values of

the inter-dot distance corresponding to different quantum phases. Here \downarrow represents the minority spins. For $d < d_a$ (left column), it is indeed apparent that the pair correlation function is the same when both electrons are in the same dot [$z' = z'' = z_1$, panel (a)] or on different dots [$z' = z_1$ and $z'' = z_2$, panel (b)]. In this sense, the system behaves ‘coherently’. For $d > d_b$ (right column), the maps indicate that the probability of finding two \downarrow -electrons in the same dot is negligible, consistently with the picture of isolated dots. In the intermediate phase $d_a < d < d_b$ this is no longer the case: the electronic wavefunctions extend over both dots, and the $g_{\downarrow,\downarrow}$ pair correlation functions are very different depending on the location of both electrons in the same or in different dots. Note that transitions between different electronic configurations vs. d were recently identified theoretically also for classical coupled dots [10]: We find that, for the small values of N considered here, the number of distinct phases and the spatial distribution of electrons (as reflected in their correlation functions) is drastically modified by quantum effects.

The above findings are expected to be observable experimentally. First, the calculated magnetic-field dependent addition spectra $A(N)$ present clear signatures of the phase transitions described above, as illustrated in Fig. 4. Here $A(N) = E(N) - E(N - 1)$ is obtained from the many-body ground state energies of the N - and $(N - 1)$ -electron systems, on the basis of single-particle states calculated in the presence of the external magnetic field B . The behaviour shown in the left, central, and right panels is representative of the three phases. Secondly, the changes in the magnetization induced by one electron addition —also accessible experimentally [11]— are expected to follow a different pattern in each phase (see the different sequence of quantum numbers in Fig. 2).

A large experimental effort is presently devoted to transport experiments in double QDs. In most cases, the dots are obtained by gating a two-dimensional electron gas (lateral confinement), and their coupling can be tuned through a gate voltage [11–15]. Indeed, a set of experiments has recently demonstrated a clear transition to a ‘coherent’ state with increasing coupling between dots [13,15]. Outside this strong coupling regime, however, experiments performed in the lateral geometry have so far evidenced classical interdot capacitance effects, probably owing to the size of dots [16]. On the other hand, transport experiments are now available on DQD structures with strong lateral confinement fabricated by combined growth and etching techniques [5,17]. The advantage is that the number of electrons in the structure is limited, while an accurate control on the inter-dot coupling is still possible by designing samples with appropriate barrier thickness. Both aspects are important to enhance many-body effects and to explore intermediate coupling regimes. Recent experimental work on these structures has focused on the weak-coupling regimes [5]. We hope that further investigations will be stimulated by the present work, since the relevant transitions are now

predicted quantitatively and should occur in a range of parameters that is accessible to state-of-the-art experiments. We expect that such studies will bring new insight into electron-electron interaction effects in coupled quantum nanostructures.

We acknowledge helpful discussions with C. Calandra and G. Goldoni. This work was supported in part by INFN PRA99-SSQI, by the EC under the TMR Network “Ultrafast Quantum Optoelectronics”, and by the MURST-40% program “Physics of Nanostructures”.

-
- [1] For reviews see: R.C. Ashoori, *Nature* **379**, 413 (1996); L.P. Kouwenhoven et al., in *Mesoscopic Electron Transport*, edited by L. Sohn et al. (Kluwer, Dordrecht, 1997); and references therein.
 - [2] L. Jacak, P. Hawrylak, and A. Wójs, *Quantum Dots* (Springer, Berlin, 1998).
 - [3] K.A. Matveev et al., *Phys. Rev.* **B53**, 1034 (1996); J.M. Golden and B.I. Halperin, *Phys. Rev.* **B56**, 4716 (1996).
 - [4] Hubbard-like hamiltonians for QDs are also used — with different levels of approximations — in G.W. Bryant, *Phys. Rev.* **B48**, 8024 (1993); G. Klimeck et al., *Phys. Rev.* **B50**, 2316 (1994); J.J. Palacios et al., *Phys. Rev.* **B51**, 1769 (1995); R. Kotlyar and S. Das Sarma, *Phys. Rev.* **B56**, 13235 (1997); Y. Asano, *Phys. Rev.* **B58**, 1414 (1998); Y. Tokura et al., *Proc 24th Internat. Conference on the Physics of Semiconductors*, edited by D. Gershoni, World Scientific (1999), in press.
 - [5] D.G. Austing et al., *Jpn. J. Appl. Phys.* **36**, 1667 (1997).
 - [6] S. Tarucha et al., *Phys. Rev. Lett.* **77**, 3613 (1996).
 - [7] The same approach was introduced for the case of isolated QDs giving addition spectra in good agreement with experiments [M. Rontani, F. Rossi, F. Manghi, and E. Molinari, *Appl. Phys. Lett.* **72**, 957 (1998); *Phys. Rev. B* **59**, 10165 (1999)]. In that case, however, the Hubbard hamiltonian reduces to an effective one-body hamiltonian since t and the inter-dot integrals are zero.
 - [8] Ground state configurations are labeled in the molecular notation: $\Sigma, \Pi, \Delta, \Phi, \Gamma, I$ correspond to $M = 0, \dots, 5$; the left superscript is $2S + 1$; g and u specify the symmetry under inversion with respect to the center of the molecule; $+$ and $-$ the symmetry under the $z \rightarrow -z$ reflection.
 - [9] M. Eto, *Solid State Electronics* **42** 1373 (1998)
 - [10] B. Partoens et al., *Phys. Rev. Lett.* **79**, 3990 (1997).
 - [11] T.H. Oosterkamp et al., *Phys. Rev. Lett.* **80**, 4951 (1998).
 - [12] F.R. Waugh et al., *Phys. Rev. Lett.* **75**, 705 (1995).
 - [13] C. Livermore et al., *Science* **274**, 1332 (1996).
 - [14] T.H. Wang and S. Tarucha, *Appl. Phys. Lett.* **71**, 2499 (1997).
 - [15] R.H. Blick et al., *Phys. Rev. Lett.* **80**, 4032 (1998).
 - [16] Interesting deviations from predictions of simple capacitance models are however reported in Refs. [11,12].
 - [17] DQD with different geometries, obtained by cleaved-edge or self-organized growth, have recently become available

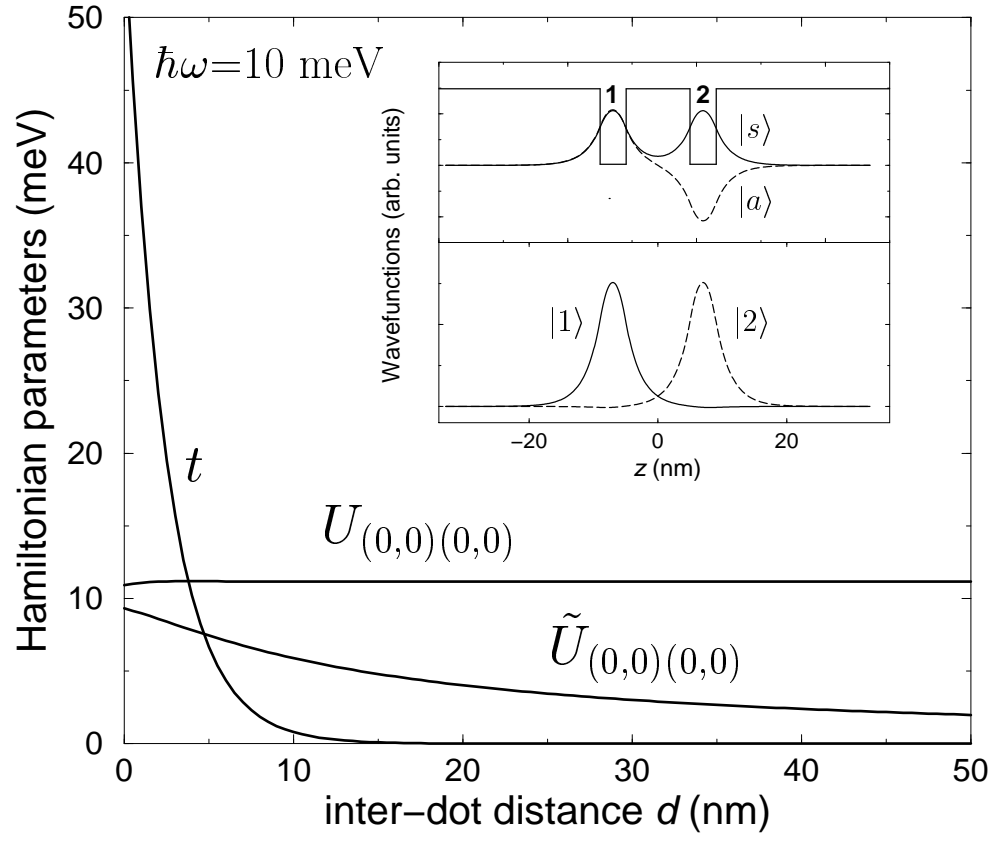
but were so far investigated mostly by optical experiments. See e.g. G. Schedelbeck et al., *Science* **278**, 1792 (1997); N.N. Ledentsov et al., *Phys. Rev. B* **54**, 8743 (1996); R. Cingolani et al. (1999), unpublished.

FIG. 1. Parameters entering the many-body Hamiltonian of a double quantum dot with $\hbar\omega = 10$ meV, plotted as a function of the interdot distance d . The hopping coefficient t is shown together with two of the intra-dot and inter-dot Coulomb integrals. In the inset, the top panel shows the confinement potential $V(z)$ (the barrier height is 200 meV) and the corresponding symmetric and antisymmetric single-particle wavefunctions, $|s\rangle$ and $|a\rangle$; the bottom panel displays the localized states, $|1\rangle$ and $|2\rangle$, obtained as combinations of $|s\rangle$ and $|a\rangle$, that are used as basis set for our calculation.

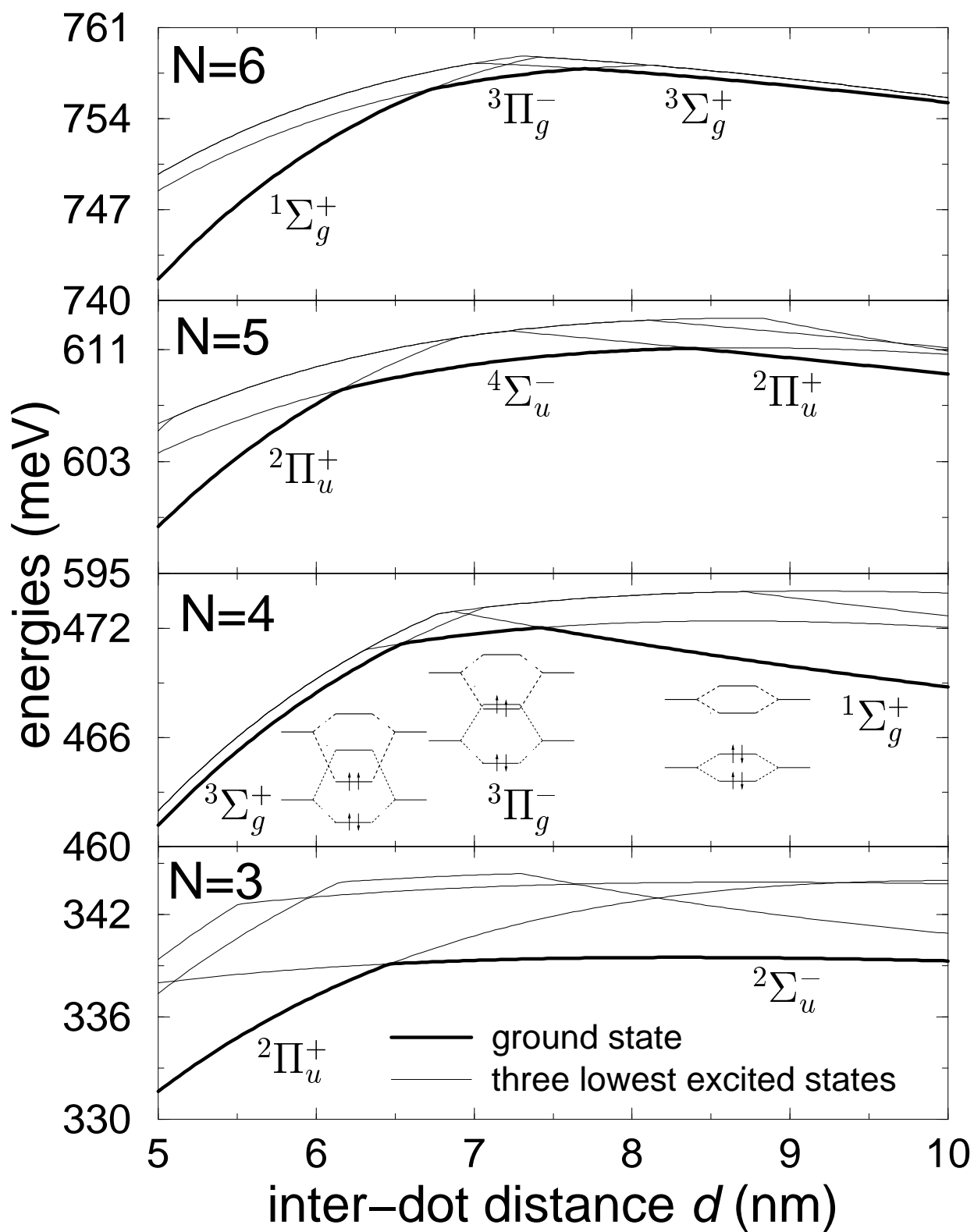
FIG. 2. Energies of the ground state (thick line) and three lowest excited states (thin lines) as a function of the inter-dot distance, d , for a double QD occupied by N electrons. For $N = 4$, the prominent single particle configurations contributing to the many-body ground state are shown in the insets. Note that in the intermediate phase a significant contribution comes also from other Slater determinants (see text). The π molecular states are doubly degenerate because of the two-fold degeneracy of the second shell in the single-dots (p_x, p_y).

FIG. 3. Electronic pair correlation functions for a double QD with $N = 6$ electrons, calculated at three values of the inter-dot distance, d , corresponding to the different quantum phases. The maps are plotted as a function of the difference between the in-plane coordinates of the electrons in the pair ($x = x' - x''$ and $y = y' - y''$), while their z coordinates are fixed either at the center of the same dot [$g_{\downarrow,\downarrow}(x, y, z_1, z_1)$; upper panels] or at the center of different dots [$g_{\downarrow,\downarrow}(x, y, z_1, z_2)$; lower panels]. Here \downarrow represents the minority spins.

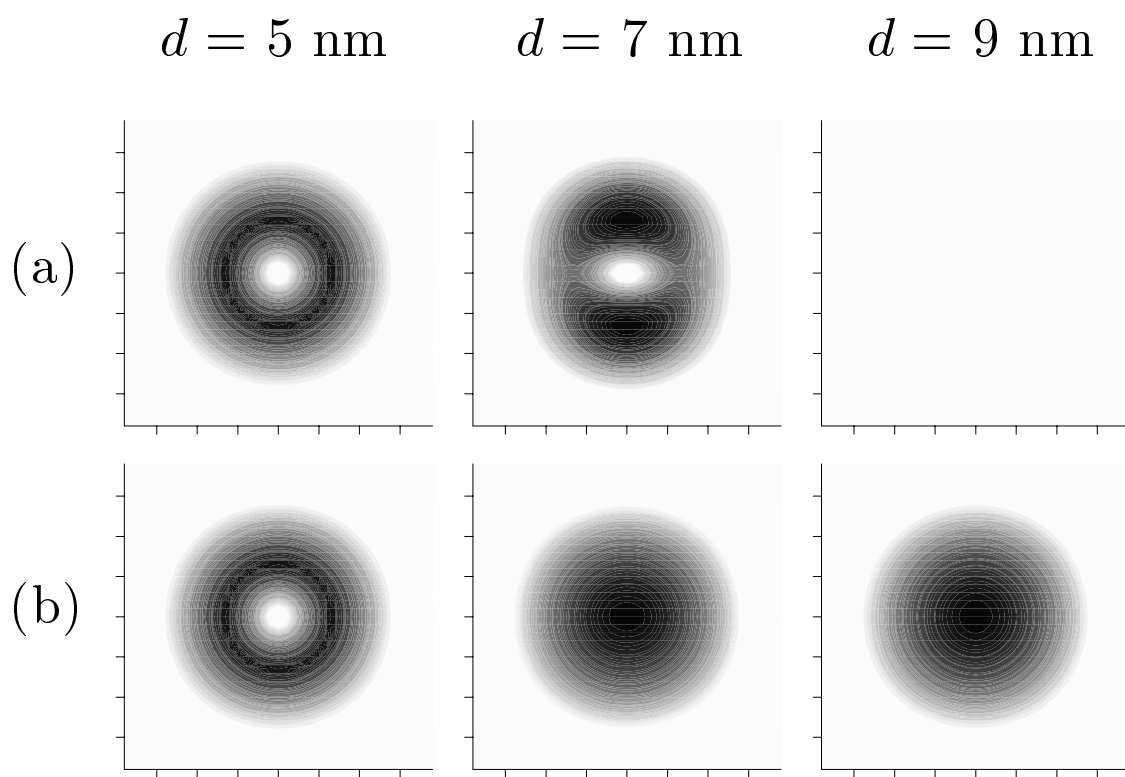
FIG. 4. Calculated addition spectra, $A(N) = E(N) - E(N - 1)$, as a function of magnetic field B for a double QD, calculated at three values of the inter-dot distance, d , corresponding to the different quantum phases. Labels indicate the ground state configuration of the N -electron system. The energy zero is arbitrary.



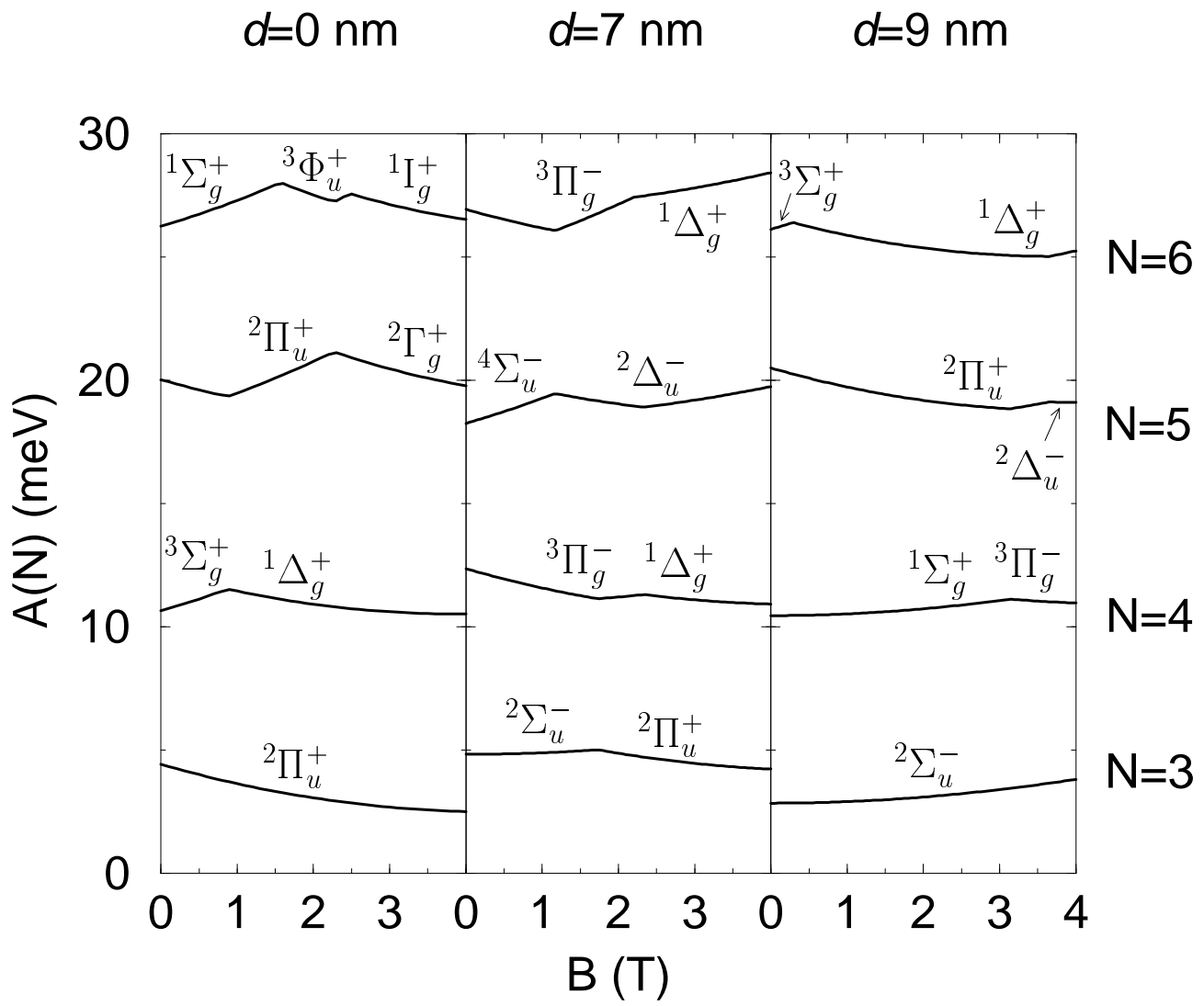
M. Rontani *et al.*: Fig. 1



M. Rontani *et al.*: Fig. 2



M. Rontani *et al.*: Fig. 3



M. Rontani *et al.*: Fig. 4